Resonant spin amplification of resident electrons in CdTe/(Cd,Mg)Te quantum wells subject to tilted magnetic fields

E. A. Zhukov,[1] O. A. Yugov,[1,2] I. A. Yugova,[1,2] D. R. Yakovlev,[1,3]
G. Karczewski,[4] T. Wojtowicz,[4] J. Kossut,[4] and M. Bayer[1]
[1]*Experimentelle Physik 2, Technische Universität Dortmund, 44221 Dortmund, Germany*
[2]*St. Petersburg State University, 198504 St. Petersburg, Russia*
[3]*Ioffe Physical-Technical Institute, Russian Academy of Sciences, 194021 St. Petersburg, Russia*
[4]*Institute of Physics, Polish Academy of Sciences, 02668 Warsaw, Poland*
(Received 24 August 2012; revised manuscript received 24 September 2012; published 17 December 2012)

Electron spin coherence in CdTe/(Cd,Mg)Te quantum wells is studied experimentally and theoretically in tilted external magnetic fields generated by a superconducting vector magnet. The long-lived spin coherence is measured by pump-probe Kerr rotation in the resonant spin amplification (RSA) regime. The shape of RSA signals is very sensitive to weak magnetic field components deviating from the Voigt or Faraday geometries.

DOI: 10.1103/PhysRevB.86.245314 PACS number(s): 78.67.De

Resonant spin amplification (RSA) is a pump-probe technique used for the study of carrier spin coherence when the spin relaxation time is comparable to or longer than the laser repetition period.[1,2] In RSA experiments the delay between pump and probe pulses is fixed (usually at a small negative delay of the probe pulse relative to the pump pulse) and spin polarization is measured as a function of the magnetic field oriented orthogonal to the optical excitation (Voigt geometry). Increasing the magnetic field changes the Larmor frequency of the electron spin precession about the field direction. At some field strengths, at which an integer number of revolutions during the Larmor precession lasts equally as long as the repetition period of the pump pulses, the electron spin polarization accumulates efficiently. The resulting RSA spectrum is a periodic function of the magnetic field with sharp peaks corresponding to these resonance fields.

The RSA technique has been successfully used for the investigation of bulk GaAs as well as III-V and II-VI quantum wells (QWs).[1–8] This technique is very sensitive both to the properties of the studied spin systems and to the experimental conditions (strength and orientation of the magnetic field, temperature, excitation density, etc.). As a result the shape of RSA spectra can vary considerably—see Ref. 8 and references therein. However, if analyzed with care, RSA spectra allow one to determine with high accuracy the spin relaxation times and g factors and to obtain comprehensive information about the generation and relaxation of carrier spin coherence. For example, it has been suggested theoretically[9] and recently shown experimentally[10] that the ratio of the zero-field and the adjacent, finite-field RSA peak amplitudes can be used for the evaluation of the spin relaxation time anisotropy in QWs.

As the RSA peak widths may be smaller than a millitesla, the shape of the RSA spectrum can be strongly influenced by additional magnetic fields of comparable strength deviating from the nominal Voigt geometry. Resident magnetic fields in superconducting solenoids could be the origin of disturbing fields of a few millitesla strength. While such instrumental fields may be avoided, there could be also sample-inherent fields such as the exchange fields of the nuclear spins or magnetic impurities that may contribute to the carrier Zeeman splitting, acting as an effective magnetic field with orientation different from the external one. The Dresselhaus and Rashba spin splitting of the conduction band electrons, caused by the spin-orbit interaction, results also in an effective exchange field with orientation given by the carrier wave vector.[11] These additional fields may distort the RSA spectra, complicating their interpretation. Vice versa, such distortions may also open new possibilities: If well understood, such distortions may be used to obtain insight into additional internal fields beyond the external field. This approach was used for bulk GaAs to obtain insight into the internal effective magnetic field, induced by an external electric field.[12,13] For comprehensive insight the effects of a tilted magnetic field need to be understood in detail. Despite a considerable number of studies using the RSA technique, measurements performed in tilted magnetic field geometry are rare and were used only for investigating carrier g-factor anisotropies.[6] A detailed analysis of the RSA shape for these appealing experimental conditions is still missing.

In this paper we study experimentally and theoretically the effect of magnetic fields tilted on purpose on the RSA signal shape. The experiments address the long-lived spin coherence of resident electrons in CdTe/(Cd,Mg)Te QWs, which is a well-studied heterostructure for which most of the spin-related parameters are precisely known. In addition, nuclear spin effects in these QWs are much less pronounced than in III-V structures. Therefore we use this rather pure model system for testing the effect of tilted magnetic field components on the RSA spectra. This knowledge may allow one to conclude about internal fields in other less understood systems.

The studied CdTe/$Cd_{0.63}Mg_{0.37}$Te quantum well structure (090505AC) was grown by molecular-beam epitaxy on a (100)-oriented GaAs substrate with a 4 μm $Cd_{0.75}Mg_{0.25}$Te buffer layer. The structure contains a 20-nm-thick CdTe single QW separated from the buffer layer by a 150-nm-thick $Cd_{0.63}Mg_{0.37}$Te barrier and from the surface by a 120-nm-thick $Cd_{0.63}Mg_{0.37}$Te barrier. The sample is nominally undoped but due to residual impurities and charge redistribution to surface states the QW at low temperatures contains low concentrations of resident electrons and holes not exceeding 10^{10} cm^{-2}.[14,15] These resident carriers are spatially separated in the QW plane. As the hole spin dephasing time of 500 ps is considerably

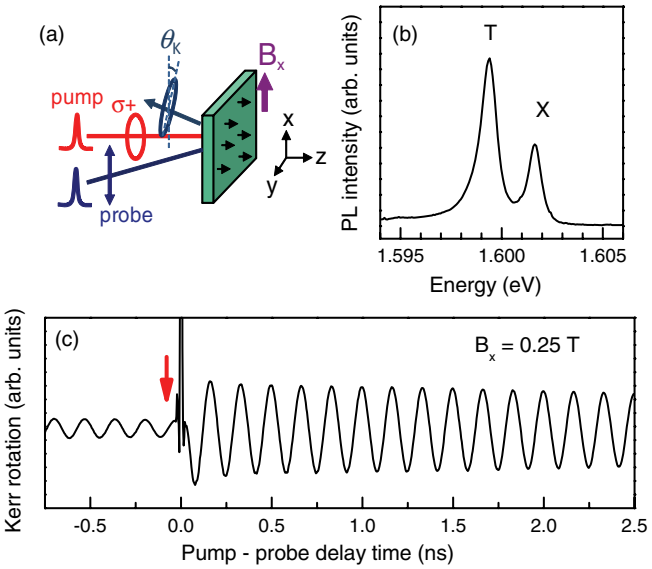

FIG. 1. (Color online) (a) Scheme of the pump-probe Kerr rotation experiment in the Voigt geometry. (b) Photoluminescence of the CdTe/$Cd_{0.63}Mg_{0.37}$Te QW. T and X mark trion and exciton resonances at 1.5995 and 1.6017 eV, respectively. $T = 1.8$ K. (c) Time-resolved KR signal measured in transverse magnetic field (Voigt geometry) for optical excitation of the exciton resonance. The arrow shows the probe arrival time for RSA measurements.

shorter than the laser repetition period $T_R = 13.2$ ns, the RSA signals in these QWs are solely contributed by the resident electrons with long-lived spin coherence. Figure 1(b) shows the photoluminescence spectrum of the studied QW measured at $T = 1.8$ K. The two emission lines correspond to the exciton (1.6017 eV) and the trion (1.5995 eV) optical transitions.

The spin dynamics was measured by a time-resolved pump-probe Kerr rotation (KR) technique based on a mode-locked Ti:sapphire laser generating 1.5 ps pulses at a repetition frequency of 75.6 MHz (repetition period $T_R = 13.2$ ns). Electron spin coherence was generated along the growth axis **z** by the circularly polarized pump pulses—see Fig. 1(a). An elasto-optical modulator operated at a frequency of 50 kHz was used for polarization of the pump beam. In order to avoid electron heating and delocalization effects the pump density was kept low at a level of 2 mW/cm^2. The probe beam was linearly polarized and the angle of its Kerr rotation after reflection from the sample, θ_K, was measured by a balanced photodetector. Pump and probe beams had the same photon energy and were tuned to the energy of the exciton resonance. For the RSA experiments presented here the probe pulse arrival moment was set to a small negative delay time ($\Delta t = -50$ ps), i.e., slightly prior to the pump pulse arrival.

The sample was placed in a vector magnet system consisting of three superconducting split coils oriented orthogonally to each other. This magnet system allows one to ramp a magnetic field parallel or perpendicular to the structure growth axis, $\mathbf{B} \parallel \mathbf{z}$ or $\mathbf{B} \perp \mathbf{z}$ (Faraday or Voigt geometry), and also apply an additional, constant field component along other directions.[16] An important advantage of the vector magnet is the possibility of complete compensation of residual magnetic fields, which are inherent for superconducting coils due to frozen currents. Such compensation on a level of better than 0.2 mT was important for the performed experiments. The sample was immersed in pumped liquid helium and kept at a temperature of $T = 1.8$ K.

Figure 1(c) shows a time-resolved Kerr rotation signal measured in Voigt geometry $\mathbf{B} \parallel \mathbf{x}$ at $B_x = 0.25$ T. The oscillations in the KR signal correspond to spin precession of excess electrons with a g-factor value $|g| = 1.60$. The decay of signal amplitude is weak over the shown time interval of 2.5 ns after the pump. The appearance of an oscillating signal at negative pump-probe delays means that spin precession is maintained up to the next pump pulse arrival, i.e., that the electron spin dephasing time T_2^* is longer than the laser repetition period $T_R = 13.2$ ns. In such cases, when the spin relaxation time is equal to or longer than the laser repetition period, one can use the RSA technique to study spin relaxation processes by scanning the magnetic field at a fixed negative delay in a time range near zero.

In the Voigt geometry the RSA spectrum for the studied structure has the classical shape, containing regularly spaced peaks—see the lowest curve in Fig. 2(a). The peaks broaden and their amplitude decreases with increasing magnetic field strength due to spin dephasing caused by the inhomogeneity of the electron spin ensemble. Experimental RSA spectra in a tilted magnetic field are shown in Figs. 2(a)–2(c). For the measurements in Figs. 2(a) and 2(b) the scanned magnetic field is applied perpendicular to the structure growth axis (and to the light propagation direction) $\mathbf{B} \parallel \mathbf{x}$. Simultaneously weak constant fields of few mT strength are applied along two other directions: along the **y** axis in Fig. 2(a) and **z** axis in Fig. 2(b). Figure 2(c) shows the electron spin polarization in the scanned longitudinal magnetic field $\mathbf{B} \parallel \mathbf{z}$ (Faraday geometry). The different curves correspond to different values of weak constant fields applied along the **x** axis. One sees that even weak constant magnetic fields applied perpendicular to the scanned fields drastically change a RSA spectrum. Depending on the experimental geometry these changes resemble the disappearance of the central peak at zero field [Fig. 2(a)], broadening of the central peak [Figs. 2(a) and 2(b)], or the appearance of a dip at the center with oscillations to both sides [Fig. 2(c)].

It is intuitively understandable that the strong modifications of the RSA spectral shape shown in Fig. 2 are connected with the origin of resonant spin amplification. The width of the RSA peak at zero magnetic field is only 1.3 mT. This means that the constant field components of a few mT (which are small compared to the field strengths often applied in RSA studies), which are applied perpendicular to the scanned magnetic field, must have a considerable effect. For the zero-field RSA peak they will induce a tilt of the total magnetic field by large angles exceeding $\pi/4$. That is why the changes in the RSA spectra are so prominent. For example, the fading of the zero-field RSA peak in Fig. 2(a) with increasing B_y and its disappearance around 1.8 mT is analogous to the Hanle effect in optical orientation. The spin polarization rises again with a further increase of B_y up to 3.3 mT, at which the RSA condition is met again for one full period of Larmor spin precession between the laser pulse arrival times.

For detailed modeling of the RSA spectra we use the approach of Ref. 8 and extend it for tilted magnetic field geometries. The ensemble of electron spins is polarized by

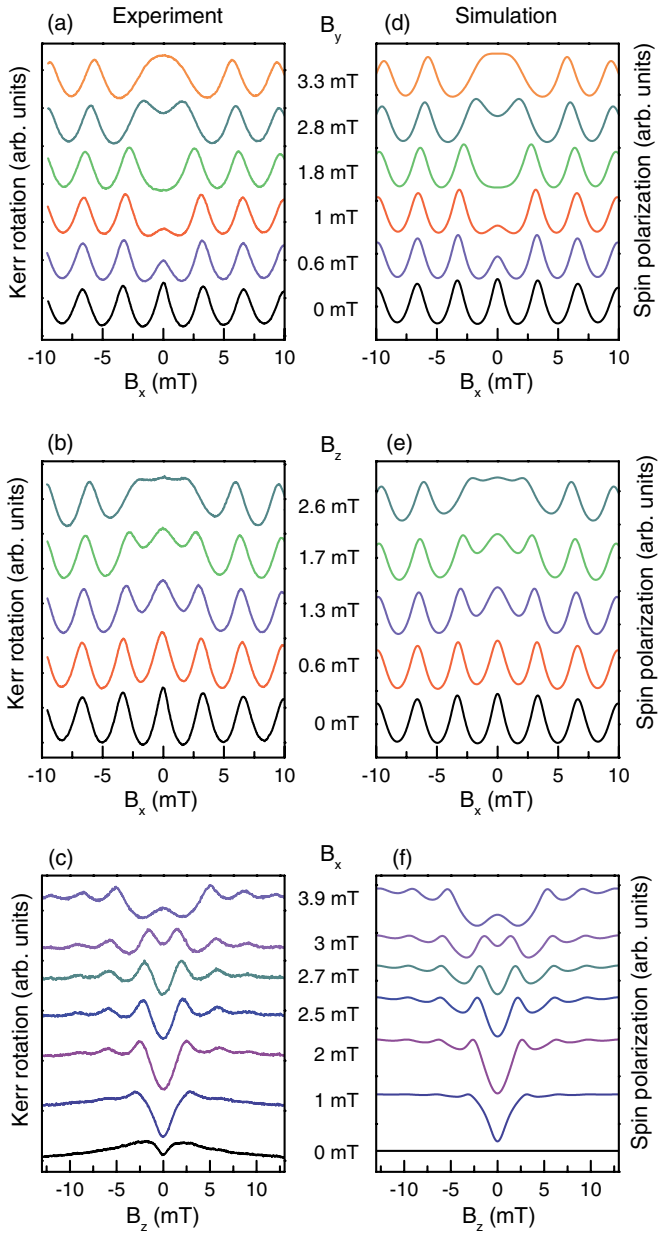

FIG. 2. (Color online) (a)–(c) Experimental and (d)–(f) calculated RSA spectra in tilted magnetic fields. $T = 1.8$ K. (a), (d) and (b), (e) show the effect of a small constant magnetic field applied perpendicular to the scanned field B_x. The strengths of these fields, B_y or B_z, are given near the corresponding experimental and theoretical curves. (c) and (f) show the electron spin polarization in RSA measured with the longitudinal component of the magnetic field scanned at small, fixed B_x.

the periodical train of laser pulses with a repetition frequency $\omega_R = 2\pi/T_R$. For simplicity we assume that the electron spin relaxation is isotropic and the electron g factor is also isotropic.[17,18] A typical RSA signal for the Voigt geometry (i.e., no tilt of the magnetic field) can be seen in Fig. 6(a) of Ref. 8. It consists of a sequence of peaks located at the specific magnetic fields determined by the electron g factor and the laser repetition frequency, $B_N = N\hbar\omega_R/(|g|\mu_B)$. Here N is an integer, $\hbar$ is Planck's constant, and μ_B is the Bohr magneton. The RSA peak width is determined by the spin coherence time T_2 for a homogeneous ensemble of electron spins or by the spin dephasing time T_2^* for an inhomogeneous spin ensemble.

The generation of electron spin polarization by the pump pulse is described by the following equations:

$$S_z^a = \frac{Q^2-1}{4} + S_z^b\frac{Q^2+1}{2}, \tag{1a}$$

$$S_x^a = QS_x^b, \tag{1b}$$

$$S_y^a = QS_y^b. \tag{1c}$$

Here $\boldsymbol{S}^b$ and $\boldsymbol{S}^a$ are the electron spin polarizations before and after the pump pulse, respectively. $Q = \cos(\Theta/2)$ with Θ being the pulse area. In order to account for the periodical excitation by the train of pump pulses we combine Eqs. (1) with the equation that describes the time evolution of the electron spin dynamics between the pump pulses and also accounts for the tilted magnetic fields:

$$\begin{aligned}\boldsymbol{S} = {} & [\boldsymbol{n}(\boldsymbol{n}\cdot\boldsymbol{S}^a) + (\boldsymbol{S}^a - \boldsymbol{n}(\boldsymbol{n}\cdot\boldsymbol{S}^a))\cos(\omega t) \\ & + [\boldsymbol{S}^a - \boldsymbol{n}(\boldsymbol{n}\cdot\boldsymbol{S}^a)]\times\boldsymbol{n}\sin(\omega t)]\exp(-t/T_2),\end{aligned} \tag{2}$$

where $\boldsymbol{n} = \boldsymbol{B}/B$ is a unit vector along the magnetic field and $\omega = |g|\mu_B B/\hbar$ is the electron Larmor precession. Then we calculate the accumulated spin polarization after a train of pump pulses demanding that the carrier spin after each repetition period $\boldsymbol{S}(T_R)$ [given by Eq. (2)] should be equal to the spin right before the pump pulse arrival $\boldsymbol{S}^b$ [given by Eqs. (1)]. We assume here that, as is typical for QWs, the inhomogeneity of the electron spin ensemble is implemented by a spread of Larmor frequencies, which on the other hand is due to a g-factor spread. Following the approach of Sec. III D 1 from Ref. 8 we assume that the g-factor spread distribution function is Gaussian with a mean value g_0 and dispersion Δg. The corresponding Larmor frequency precession spread is $\Delta\omega(B) = \Delta g\mu_B B/\hbar$. To model the ensemble RSA signal we sum the contributions of the individual spins over the g-factor distribution function.

Illustrative model results calculated with the following parameters, $T_2 = T_R$, $\Theta = 0.1\pi$, and $\Delta\omega = 0.05\omega$, are shown as two-dimensional contour plots in Figs. 3 and 4. Figure 3 presents the dependence of the RSA spectrum on the two transverse components of the magnetic field, B_x and B_y. The RSA signal amplitude is shown in grayscale, where bright regions correspond to maximal signal strength. Note that in the absence of magnetic fields ($\omega_x = \omega_y = 0$) the electron spin polarization is maximal because the electron spins do not undergo Larmor precession and the RSA condition is fulfilled for all of them. For universality, the x and y field component strengths are given in units of the corresponding Larmor frequencies $\omega_{x(y)} = |g|\mu_B B_{x(y)}/\hbar$ normalized to the laser repetition frequency ω_R. Each cut through the center of Fig. 3 with coordinates $\omega_y = \omega_x = 0$, resulting in a plot of the RSA amplitude versus magnetic field, corresponds to a single RSA spectrum. As we chose isotropic g factors and spin relaxation times in our model all orientations are equivalent to each other for these cuts so that the contour plot has a circular symmetry, with the circles of brightest intensity corresponding to RSA peaks. The circles become blurred with increasing field due to the enhanced spread of the Larmor frequency caused by Δg.

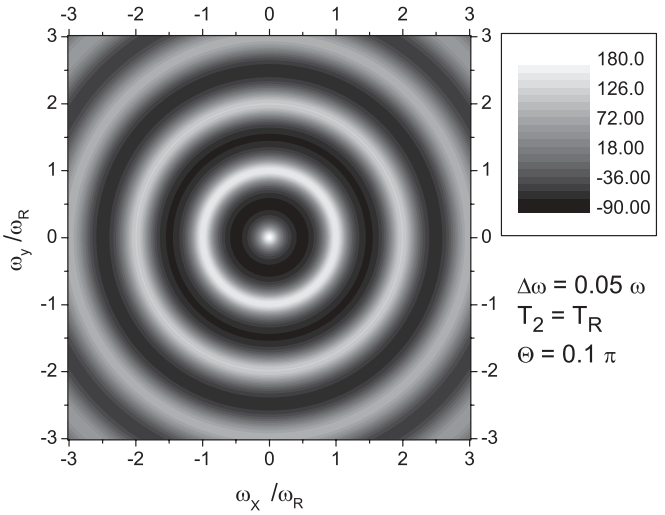

FIG. 3. RSA spectra calculated as function of magnetic field applied in the plain of the $\{xy\}$ sample plain (Voigt geometry). The RSA signal strength is color coded according to the grayscale on the right-hand side.

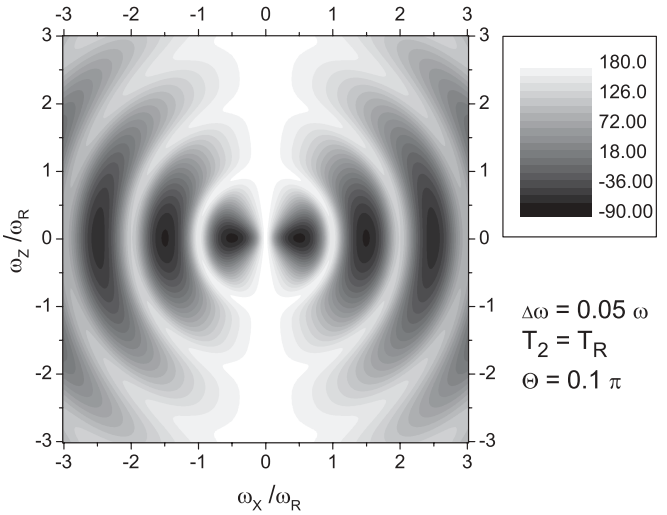

FIG. 4. RSA spectrum calculated in dependence of the magnetic field applied in the $\{zx\}$ plain (going from the Faraday to the Voigt configurations). The RSA signal strength is is color coded according to the grayscale on the right-hand side.

Figure 4 shows a two-dimensional contour plot as a function of the transverse field B_x and the longitudinal field B_z. One can see that in the presence of a longitudinal field component a region of conserved spin polarization (white area) appears. This is due to the fact that the longitudinal field component does not destroy but rather stabilizes the electron spin polarization.

In order to see how well the experimentally observed features can be reproduced by the modeling, the corresponding calculated RSA spectra are plotted in Figs. 2(d)–2(f). Most parameters for these calculation are known from experiment: $|g| = 1.60$, $\Delta g = 0.06$, $\Theta = 0.1\pi$. $T_2 = 9$ ns was a free parameter selected for best agreement with the experimental data from the left panels of this figure. The calculated spectra are in very good accord with experiment. This confirms that all parameters of the resident electron spins in our model CdTe/(Cd,Mg)Te QW are well understood. Small discrepancies between the traces in Figs. 2(c) and 2(f) can be related to (i) our experimental accuracy of the residual magnetic field compensation, and (ii) the fact that we cannot fully neglect the spin orientation mechanism in the longitudinal magnetic field dependence.[8] It is worth remembering here that the lowest RSA spectrum in Fig. 2(f) calculated for $B_x = 0$ has an amplitude corresponding to maximal electron polarization. And this polarization is not affected by the longitudinal magnetic field B_z—see also Fig. 4.

In conclusion, we performed detailed experimental and theoretical studies of the effect of the magnetic field orientation on the RSA spectra of resident electrons in semiconductor QWs. It was found that already weak magnetic field components of a few mT only, being oriented perpendicular to the scanned magnetic fields in the Voigt or Faraday geometries, can strongly modify the RSA spectra, especially around the zero-field RSA peak. This result is important and instructive for applying the sensitive RSA technique to the investigation of carrier spin dynamics: Considerable care needs to be exercised in aligning the external magnetic field and compensating and/or accounting for field components deviating from the Voigt geometry. Any such deviations might lead to deceptive results when measuring the anisotropy of the spin relaxation time, spin orientation mechanism, or carrier hyperfine interaction with nuclear spins. Vice versa, deviations from an expected RSA shape might hint at internal exchange fields.

This work was supported by the BMBF project QuaHL-Rep, the Deutsche Forschungsgemeinschaft, the Mercur Research Center Ruhr, and the NRW-project PlusLucis. I.A.Y. is supported by a fellowship of the Alexander von Humboldt Foundation. Research in Poland was partially supported by the European Union within the European Regional Development Fund, through Innovative Economy Grant No. POIG.01.01.02-00-008/08.

[1] J. M. Kikkawa and D. D. Awschalom, Phys. Rev. Lett. **80**, 4313 (1998).

[2] *Semiconductor Spintronics and Quantum Computation*, edited by D. D. Awschalom, D. Loss, and N. Samarth (Springer, Berlin, 2002).

[3] G. V. Astakhov, M. M. Glazov, D. R. Yakovlev, E. A. Zhukov, W. Ossau, L. W. Molenkamp, and M. Bayer, Semicond. Sci. Technol. **23**, 114001 (2008).

[4] I. A. Yugova, A. A. Sokolova, D. R. Yakovlev, A. Greilich, D. Reuter, A. D. Wieck, and M. Bayer, Phys. Rev. Lett. **102**, 167402 (2009).

[5] L. V. Fokina, I. A. Yugova, D. R. Yakovlev, M. M. Glazov, I. A. Akimov, A. Greilich, D. Reuter, A. D. Wieck, and M. Bayer, Phys. Rev. B **81**, 195304 (2010).

[6]T. Korn, M. Kugler, M. Griesbeck, R. Schulz, A. Wagner, M. Hirmer, C. Gerl, D. Schuh, W. Wegscheider, and C. Schüller, New J. Phys. **12**, 043003 (2010).

[7]M. Kugler, K. Korzekwa, P. Machnikowski, C. Gradl, S. Furthmeier, M. Griesbeck, M. Hirmer, D. Schuh, W. Wegscheider, T. Kuhn, C. Schüller, and T. Korn, Phys. Rev. B **84**, 085327 (2011).

[8]I. A. Yugova, M. M. Glazov, D. R. Yakovlev, A. A. Sokolova, and M. Bayer, Phys. Rev. B **85**, 125304 (2012).

[9]M. M. Glazov and E. L. Ivchenko, Semiconductors **42**, 951 (2008).

[10]M. Griesbeck, M. M. Glazov, E. Ya. Sherman, D. Schuh, W. Wegscheider, C. Schüller, and T. Korn, Phys. Rev. B **85**, 085313 (2012).

[11]J. Fabian, A. Matos-Abiaguea, C. Ertlera, P. Stano, and I. Zutic, Acta Phys. Slov. **57**, 565 (2007).

[12]J. M. Kikkawa and D. D. Awschalom, Nature (London) **397**, 139 (1999).

[13]Y. Kato, R. C. Myers, A. C. Gossard, and D. D. Awschalom, Nature (London) **427**, 50 (2004).

[14]E. A. Zhukov, D. R. Yakovlev, M. Gerbracht, G. V. Mikhailov, G. Karczewski, T. Wojtowicz, J. Kossut, and M. Bayer, Phys. Rev. B **79**, 155318 (2009).

[15]G. Bartsch, M. Gerbracht, D. R. Yakovlev, J. H. Blokland, P. C. M. Christianen, E. A. Zhukov, A. B. Dzyubenko, G. Karczewski, T. Wojtowicz, J. Kossut, J. C. Maan, and M. Bayer, Phys. Rev. B **83**, 235317 (2011).

[16]A. Schwan, B.-M. Meiners, A. Greilich, D. R. Yakovlev, M. Bayer, A. D. B. Maia, A. A. Quivy, and A. B. Henriques, Appl. Phys. Lett. **99**, 221914 (2011).

[17]In the studied CdTe/(Cd, Mg)Te QW the anisotropy of electron g-factor is less than 2% (Ref. 18) and is insignificant for our consideration.

[18]A. A. Sirenko, T. Ruf, M. Cardona, D. R. Yakovlev, W. Ossau, A. Waag, and G. Landwehr, Phys. Rev. B **56**, 2114 (1997).